EDINBURGH INSTRUMENTS

50 YEARS 1971-2021

RMS1000

RAMAN MICROSCOPE

Extending the capabilities to Photoluminescence Microscopy, Time-Resolved Measurements and Fluorescence Lifetime Imaging (FLIM)

- Truly Confocal
- Five-Position Grating Turrets
- Two Spectrograph Options
- Up to Four Simultaneous Detectors

www.edinst.com

Received: 12 May 2021 | Revised: 17 July 2021 | Accepted: 19 July 2021

DOI: 10.1002/jrs.6217

RESEARCH ARTICLE

Journal of RAMAN SPECTROSCOPY WILEY

The potential of in situ Raman spectroscopy in the study of the health of cement-based materials of modern buildings during restoration works

Nagore Prieto-Taboada[1] | **Olivia Gómez-Laserna**[2] | **Iratxe Ibarrondo**[2] | **Irantzu Martinez-Arkarazo**[2] | **Kepa Castro**[2] | **Gorka Arana**[2] | **María Ángeles Olazabal**[2] | **Iñaki Arrieta**[3] | **Juan Manuel Madariaga**[2,4]

[1]Department of Applied Chemistry, Faculty of Chemistry, University of the Basque Country (UPV/EHU), Donostia, Basque Country, Spain

[2]Department of Analytical Chemistry, Faculty of Science and Technology, University of the Basque Country (UPV/EHU), Bilbao, Basque Country, Spain

[3]Estudio K, Getxo, Basque Country, Spain

[4]Unesco Chair of Cultural Landscapes and Heritage, University of the Basque Country UPV/EHU, Vitoria-Gasteiz, Basque Country, Spain

Correspondence
Nagore Prieto-Taboada, Department of Applied Chemistry, Faculty of Chemistry, University of the Basque Country (UPV/EHU), P° Manuel Lardizabal, 3, Donostia, Basque Country 20018, Spain.
Email: nagore.prieto@ehu.eus

Funding information
Spanish Agency for Research AEI (MICINN/FEDER-UE), Grant/Award Number: PID2020-113391GB-I00

Abstract

Although Raman spectroscopy is a common technique for the analysis of cement-based materials in the research studies or in the field of Cultural Heritage to carried out multianalytical studies, it is not generally used as unique technique of a research or to carry out analysis during ordinary restoration works of modern urban buildings affected by environmental stressors. The disadvantages associated with Raman spectroscopy as fluorescence limits its implementation beyond research studies, more in the case of in situ equipment. However, the technological development allows high-quality results with in situ equipment, so its use could be useful during restoration works. Thus, this work demonstrates how the implementation of the correct methodology could lead to useful and fast results during restoration works. The proposed methodology is based on the use of in situ analysis (screening) on the scaffolding, followed by the sampling of layers based on the previous screening and a posterior exhaustive laboratory analysis. The research has been conducted during the restoration works of a reinforced concrete building in which the attack of atmospheric acid gases (CO_2, SO_2, and NO_x) was identified as the main affection suffered, and the fixed sulfates were the most important intermediary compounds of decaying processes. Many of the pollutants and decaying compounds were even identified during the in situ analysis, improving the anticipation and responsiveness. Therefore, this methodology allows the understanding of the chemistry of the materials to evaluate its health state in a fast and reliable way.

KEYWORDS

atmospheric stressors, in situ risk assessment, restoration, scaffolding analysis, thaumasite

1 | INTRODUCTION

In restoration works of building materials affected by atmospheric stressors the awareness of the interaction between the stressors, generally the atmospheric pollution and infiltration water, and the building materials is crucial to obtain a reliable solution for its conservation.[1–5] Moreover, recent studies demonstrate that buildings can act as repositories of pollutants and affect to the human and environment during the manipulation of polluted materials.[6,7] For all of these, achieve a reliable and fast technique to be implemented for the risk assessment of the building materials, as a routine protocol in conservation works is really important to avoid problems both in the restoration quality and in the human and environment health.

In this sense, Raman spectroscopy is commonly used for the analysis of many different matrices.[8] Initially, it was more focused on inorganic compounds, but its use is growing in organic and polymer analysis.[9–11] Recent developments were the quantification of compounds and the use of spectral imaging.[12–15] However, its prevalence is undisputed in material sciences and related fields such as cultural heritage.[8,11,16,17] In this sense, the usefulness of this technique, in the analysis of construction materials and especially in concrete based materials,[18–20] has been deeply studied also to understand the interaction processes of the pollutants with them.[6,15,21–24] Furthermore, Raman spectroscopy does not need any sample preparation; it is only required a small sample and water does not interfere in the measurement. Besides, this technique differentiates between polymorphous compounds, and it is a non-destructive technique that even can be used in situ. This latter advantage is really important in conservation works, and thanks to the technological development it achieves very satisfactory results, sometimes even better than with laboratory equipment.[1,25–29]

Although Raman spectroscopy has demonstrated to be an appropriate technique for the risk assessment of building materials, nowadays, it is not used in the restoration of urban buildings, being generally employed in research studies in material science or in restoration of Cultural Heritage buildings as a part of a multianalytical research. This fact could be linked to some of the problems inherent to this technique, as the weakness of the Raman scattering effect, low sensitivity, highly optimized instrumentation needed, and the lack of adequate Raman instruments to work in the scaffolding. Moreover, some effects such as fluorescence could mask the signals because it is much higher than Raman scattering.[8,21,26] In addition, sometimes the analyses are not very representative because it is a micro-analysis technique. All of these are magnified using in situ equipment because the quality of them is supposed to be worst.

However, it is demonstrated how the technological evolution of these equipment lead to high quality results,[30] even using outside the lab[31–34] being in theory one of the best techniques to evaluate the "health" of the materials. Thus, the mentioned difficulties are not limitations, but they must be taken into account in order to avoid them. Usually, they could be overcome by complementation of Raman spectroscopy with other techniques, typically based on spectroscopy, among others, micro-X-ray fluorescence (μ-XRF), Fourier Transform infrared spectroscopy (FTIR), scanning electron microscopes (SEM), and micro-X-ray diffraction (XRD).[35–39] Nevertheless, the use of more than one technique requires a higher spending time and a greater effort to obtain valuable information, which leads to an increase of the analysis costs that, in urban buildings conservation works, is one of the most important variables. Moreover, the sampling and the use of many techniques also increase the reaction time and cost to evaluate the health of the materials.

For all of this, in order to achieve a useful and fast methodology for the in situ risk assessment of urban buildings under restoration and, thus, to demonstrate the utility of the new generation of Raman instruments for being used in conservation works (in situ analysis on the scaffolding) of urban buildings not related with Cultural Heritage, without another complementary technique, this work proposes a new methodology to solve those inconveniences. This methodology consists on the combination of an in situ analysis of the selected areas (screening), a sampling in layers based on the results of the in situ analysis and a subsequent exhaustive laboratory analysis of the samples. In this way, the previously mentioned limitations of Raman spectroscopy are expected to be minimized by the sampling based on the results of the in situ analysis. This will guarantee the representativeness of the destructive sampling, reducing the impact generated to the building as no unnecessary samples are collected. Also, the separation of samples in different layers has demonstrated to obtain valuable information of the decaying processes, thanks to the isolation of different deterioration degrees.[15]

Moreover, the ambiguity and other problems in the spectra identification may be overcome by defining some simple guidelines obtained after this study. On the whole, this protocol is aimed to reduce the effort needed to obtain the desired data, maximizing the information achieved by Raman spectroscopy pointing out its utility in real rehabilitation works of concrete based materials, leaving aside its strictly use in research works.

2 | MATERIALS AND METHODS

2.1 | Instrumentation

In the present work, an InnoRaman™ ultramobile Raman spectrometer (B&WTEK^{INC}, Newark, USA) was used to perform in situ analyses, as well as laboratory analyses at microscopic level. In the first case, the signal was transmitted by an optic fiber connected to the probe which collected the response directly above the sample. However, in the second case, the probe is connected to a stage for microscopy, having long-range objectives that focused with magnifications of 20X and 50X, which were also connected to a microcamera to view the spot under analysis. In both cases, the excitation wavelength was 785 nm (nominal laser power 255 mW), and the dispersed Raman signals were measured by a Peltier cooled CCD detector. The spectrometer was daily calibrated against a silicon chip using the 520 cm^{-1} Raman line.

The spectra were collected in the wavenumber range of 3,000–100 cm^{-1} (nonchangeable) with a spectral resolution of 3.5 cm^{-1}. Data acquisition was carried out by the BWSpec 3.26_38 software package, and the analysis of the results was undertaken by the Omnic 7.2 software (Nicolet). The e-visart and e-visarch dispersive Raman and FT-Raman spectral databases were used during the interpretation of the results.[40,41]

2.2 | Studied building and in-situ analysis points

The studied building is a reinforced concrete building covered by face bricks, constructed in the 1980s in the city of Donostia (Basque Country, North of Spain), used as the Teacher-Training School of the University of the Basque Country (UPV/EHU). The construction, located on the west of the town, is near Ondarreta beach, and close to its south facade, there is Tolosa avenue: a road with important traffic affluence (see Figure S1). The building facades were totally covered by bricks that had undergone significant deterioration on its "outer skin" in recent years.

In the moment of the analysis, a scaffolding was disposed in the northeast facade which was used to carry out the in situ analysis in the 4th floor where it was possible to access to the non-restored internal part of the reinforced concrete structure, which was directly in contact with the atmosphere. Moreover, the concrete structure was traversed by beams covered by mortar, also exposed to the atmosphere. The reinforced concrete showed detachments and several deteriorations of the surface as holes, efflorescence crystals, and whitish areas. On the other hand, the steel structure was in view and clearly deteriorated due to the degradation processes. Some areas close to the deteriorated steel showed brown marks, presumably caused by the interaction between water and the steel. Finally, recover mortars were found darkened with detachments and also affected by a green biological colonization.

In addition, a second sampling was carried out at street level where the original bricks, some of which showed clearly deteriorations and efflorescence crystals, were accessible.

2.3 | Assisted sampling based on in situ analysis

Generally, the sampling methodology of a building starts with a visual examination to discover affected areas of the surface. After that, the sampling consists of taking the fewest number of samples with the aim of avoiding the deterioration of the building but just enough to determine the affection suffered. For this purpose, the sampling of evident deterioration is carried out together with original material in order to compare their composition. However, this kind of sampling does not ensure the spectroscopic quality of the samples, and what is more, this fact could discriminate relevant areas of the study if they had not been visually detected. All of this would generate a non-representative sampling that could lead to incorrect or incomplete conclusions of the affections suffered.

For these reasons, in this work, an assisted sampling was performed thanks to the previous in-situ analysis. Thereby, the results obtained with it allowed samples with Raman signal to be collected and identify the interesting areas. This step reduced the impact caused to the building by sampling since it avoided useless sample collection.

A sampling in layers was carried out to obtain the maximum information of each sample. Therefore, when it was possible, up to three different parts of deteriorations were collected separately and not as a unique sample. For example, in samples with efflorescences, the salts were first collected without any building material. Afterwards, the most external part of the material was sampled. And finally, the innermost part of the building material without visible deterioration was collected. In this way, different steps of the decaying processes were isolated for the analysis (see Figure S2).

Regarding to the collected samples, two different areas of the building were sampled (on scaffolding and at street level). In the first one, 11 samples of steel chips, concrete, and mortar were collected. In the second sampling point, six more samples were collected of three

different materials: concrete, mortar, and brick. In both cases, a scalpel, a chisel, and a hammer were used to extract the samples that subsequently were collected in zip bags.

3 | RESULTS AND DISCUSSION

3.1 | In situ analysis

Generally, calcite ($CaCO_3$, identified by its Raman bands at 1,086, 713, 279, and 153 cm^{-1}) was found in different materials and deteriorations as mortars, efflorescences, whitish areas in concrete, and white crusts on the steel. Although calcite is a typical mineral that can be present as original compound, its presence as efflorescences, crust, or whitish areas (decaying signals) indicated that it was caused by the carbonation of the original calcium hydroxide ($Ca[OH]_2$) by the action of atmospheric CO_2. Although the generation of carbonate due to the cement hydration reaction is a beneficial process since it generates a compound that decreases porosity and increases mechanical strength, when it occurs at the interface of the cement with the reinforcement, it reduces the pH and increases the chances of corrosion of the reinforcement. This effect is known as carbonation of the concrete and involves the chemical instability of the reinforced steel promoting its oxidation and therefore, the decaying of the whole structure.

Raman spectroscopy analysis on steel structure of the reinforced concrete revealed the presence of a mixture of iron (III) oxohydroxides: lepidocrocite (γ-FeO [OH], easily identified by a strong Raman band at 255 cm^{-1}) and goethite (α-FeO [OH], characterized by the main Raman band at 382 cm^{-1}) as can be seen in Figure S3. Both compounds are connected with the oxidation of the steel (Fe°) by the action of water and oxygen infiltration through the deteriorated concrete. This reaction promotes the cracking of the material owing to the formation of iron oxides which have a bigger volume than the original steel and thereby it generates a mechanical stress inside the concrete. Hence, at the same time, the oxidation processes increase the deterioration of the concrete and it makes the filtration of oxidant agents to the steel easier, and its decay is enhanced.

On the other hand, the analysis of the reinforced concrete revealed the presence of gypsum ($CaSO_4{\cdot}2H_2O$, identified by the main Raman band at 1,007 cm^{-1}), in a fractured whitish area. This compound is an essential component in cements to control the setting time. It can be found as gypsum or can be dissolved releasing reactive $SO_4^{=}$ ions that form efflorescences of sulfated nature.[42] Furthermore, by action of the polluted atmospheres rich in SO_2, calcite can also form gypsum. In the same way, aphthitalite ($K_3Na[SO_4]_2$, detected by its Raman bands at 992 and 451 cm^{-1}) was found, and its presence could be commonly confused with thenardite since it has also the main Raman bands at 992 and 450 cm^{-1}. However, the relative intensity between these bands is not the same in both compounds, and for that reason, it was possible to distinguish aphthitalite.[43] The correct determination of such salts is really important since the worst damage level is caused by thenardite. This is due to the equilibrium between thenardite and mirabilite (Na_2SO_4—$10H_2O$) that occurs, approximately, at atmospheric temperature, depending on the humidity and entails an important change of volume. This situation is analogous to the iron oxides, also promoting the crack of the materials.[44]

The identification of several sulfates as decaying compounds pointed to the action of the atmospheric acid gases, rich in SO_2, as main source of sulfate formation.

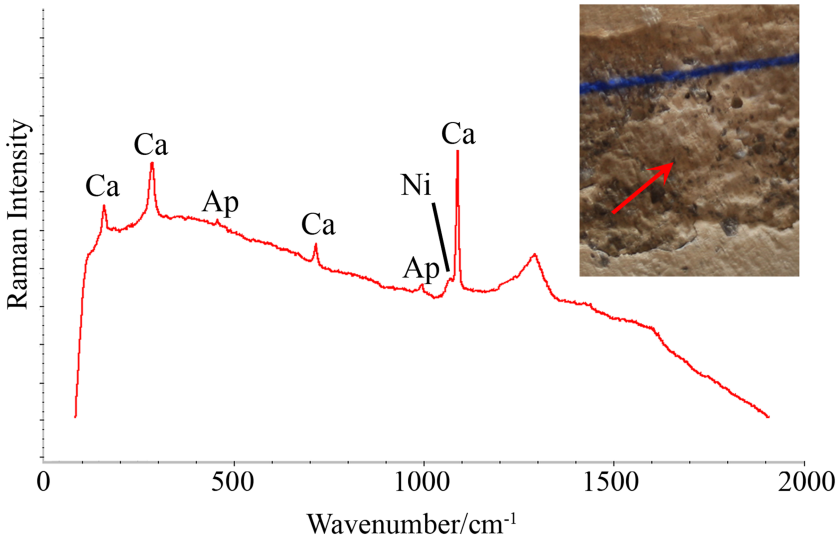

FIGURE 1 In situ Raman spectrum in which is possible identify nitratine (Ni) thanks to its main Raman band at 1,067 cm^{-1}. Moreover, aphthitalite (Ap) and calcite (Ca) can be observed [Colour figure can be viewed at wileyonlinelibrary.com]

Moreover, the material was carbonated by the atmospheric CO_2, which causes a synergistic effect of the reaction capacity of the material with other acid gases.

Finally, the identification of nitratine ($NaNO_3$) was carried out by its main Raman band at 1,067 cm^{-1} as can be seen in Figure 1, evidencing again the effect of polluted atmosphere by the action of NO_x, because of the location of the sampling point at the 4th floor of the building discards other sources of nitrates such as infiltration from soil water.[45]

3.2 | Laboratory analysis

After the described sampling, the laboratory analysis was carried to improve the spectra quality, in order to confirm the compounds previously found and even to identify others that are expected to give adequate information on the decaying sources.

First, measurements on steel chips revealed the high oxidation suffered by this material, with a better spectroscopic resolution than in situ analyses. In this way, Raman bands of lepidocrocite were identified at 643, 521, 375, 304, 248, and 214 cm^{-1} while in the case of goethite were detected at 600, 486, 398, 286, and 220 cm^{-1} (Figure S4). Besides these, a new oxide phase was found as limonite (FeO [OH]—nH_2O) identified by its Raman bands at 392 and 300 cm^{-1}.

The analysis of the interface of steel and concrete revealed two Raman bands at 1007 and 1,025 cm^{-1}, which can be seen in Figure 2a. The first band is typically related to gypsum (identified by an intense band at 1,008 cm^{-1}), and the second one, in some cases, is identified, for example, as (para-)coquimbite ($Fe_2[SO_4]_3$—$9H_2O$, detected by its main Raman band at 1,025 cm^{-1}). The formation of (para-)coquimbite depends on sulfates released by gypsum; therefore, the identification of both compounds close to an iron source (steel) is usual.[22,46] However, without the detection of secondary bands, it was difficult to certify the presence of (para-) coquimbite, as it shares the main Raman band with other compounds.[47,48]

This limitation is common in Raman spectroscopy when spectra did not showed all the secondary bands, and in these cases, it is necessary to improve the quality of them. In addition, the study of the band movements by comparison with similar spectra could avoid the use of complementary techniques. In this manner, the whole spectrum of the compound with the Raman band at 1,025 cm^{-1} was obtained, as can be seen in Figure 2b and therefore identified as soluble anhydrite ($CaSO_4$ [type III], Raman bands at 1,165, 1,025, 673, 630, 491, and 422 cm^{-1}).[48,49] The molecular structure is the main difference between the natural anhydrite (which has the main Raman band at 1,017 cm^{-1} and orthorhombic structure) and this one, which has an hexagonal structure. Another change observed was the disappearance of the band at 608 cm^{-1} due to the differences in the ν_4 flexion vibrations of the $SO_4^{=}$ group.

Moreover, other spectrum was obtained with the main Raman band at 1,011 cm^{-1} (Figure 2c) and related to a mixture of gypsum and bassanite ($CaSO_4$—$0.5H_2O$) easily observed by deconvolution analysis of the spectrum. The determination of the real calcium sulfate present in the sample is difficult because the laser power could generate the transition between metastable compounds such as bassanite and soluble anhydrite.[48] In all of these spectra, it is also possible to observe a broad

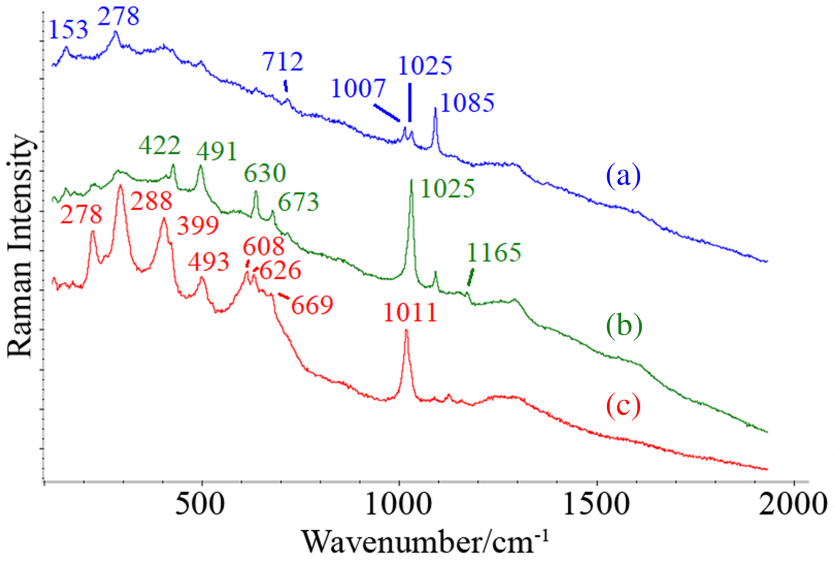

FIGURE 2 (a) Spectrum of the main Raman bands of gypsum (1,007 cm^{-1}), anhydrite III (1,025 cm^{-1}), and calcite (1,085 cm^{-1}); (b) the spectrum of soluble anhydrite with their secondary bands; and (c) a mixture of hydrated calcium sulfates, all of them in a matrix of iron oxides [Colour figure can be viewed at wileyonlinelibrary.com]

Raman band at approximately 1,300 cm^{-1} and in the Figure 2b, also at 1,600 cm^{-1}, related probably, with carbon.

Regarding the efflorescence on the mortars, a variety of sulfates were found. As it is mentioned above, the formation of such compounds was related to two formation ways. The first one consisted on the formation of sulfate compounds by reaction of carbonates with free sulfate anions from cement components. In addition, the second way caused by the reaction of carbonates with the atmospheric pollution rich in SO_2. In both cases, the formation of the efflorescences corresponded to degradation processes but with different sources, which are important to clarify. The formation of sulfates through cement components was not enough to explain their high presence. The percentage of the sulfates added to the cement could not be more than 5%; it is usually not higher than 2% due to the recent improvements in the clinker manufacture. Moreover, in the first 24 h of the setting time, this concentration decreases dramatically to form other compounds, and for this reason, the real availability of sulfates from cement components was very low.[50,51] On the other hand, taking into account the age of the building, the possibility to exude salt from the construction materials was also very improbable. For these reasons, as was indicated in the in situ analysis, the action of the atmospheric SO_2 was the most probable source of sulfates affecting to the building.

In order to understand the formation mechanism of these sulfates, the interface area of the efflorescences and mortar was studied. Thus, calcite ($CaCO_3$, identified by Raman bands at 1,085, 712, 278, and 153 cm^{-1}), gypsum ($CaSO_4$—$2H_2O$, with Raman bands at 1,134, 1,007, 670, 619, 493, and 414 cm^{-1}), and syngenite ($K_2Ca[SO_4]_2$—$2H_2O$, detected by its Raman bands at 1,164, 1,139, 1,117, 1,004, 981, 660, 641, 633, 619, 608, 492, 472, 441, and 427 cm^{-1}) were clearly identified. As can be seen in Figure 3, calcite was found in all the spectra. This fact could indicate that calcite was the starting compound for decaying reactions. In the same way, gypsum was identified in a greater number of spectra than syngenite, but it was not present when syngenite was the major compound. Thus, gypsum played as intermediate role in decaying reactions.[22,52] Therefore, this result denotes the capacity of the gypsum as a deterioration compound due to its high reactivity in degradation processes.

This hypothesis was supported by the analysis of the efflorescence crystals, which did not revealed the presence of gypsum but where syngenite and calcite were commonly detected in all of them. Besides, thenardite (Na_2SO_4, identified by its Raman bands at 1,153, 1,133, 1,103, 992, 660, 643, and 633 cm^{-1}), thaumasite ($Ca_6Si_2(OH)_{12}(CO_3)_2(SO_4)_2$—$24H_2O$, detected by Raman bands at 1,074, 990, 659, and 214 cm^{-1}), and aphthitalite ($K_3Na(SO_4)_2$, detected by its Raman band at 452 cm^{-1}) were found.

The presence of the latter compound was evidenced thanks to its second most intense band at 452 cm^{-1}. However, due to the high complexity of the spectrum, composed by several compounds, spectral treatments were carried out to confirm the presence of this sulfate, without any ambiguity. Thus, after the identification of syngenite, thaumasite, and/or calcite, the standard spectra of those compounds were subtracted from the collected spectrum. In this way, it was possible to obtain the complete spectrum of aphthitalite (characterized by its Raman bands at 992, 623, and 452 cm^{-1}) as can be seen in Figure 4.

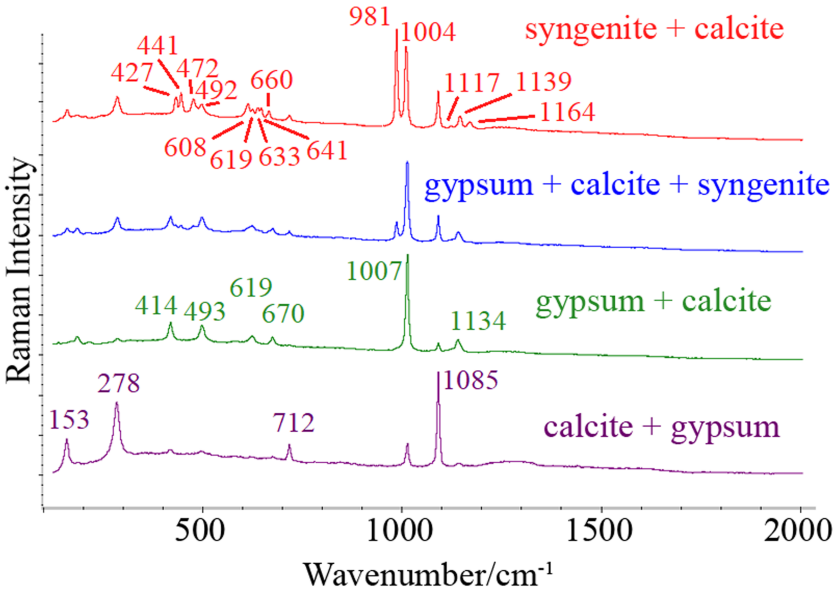

FIGURE 3 From bottom to top, it is possible to observe the spectra obtained from the interface area between an efflorescence and mortar. The formation of the syngenite from calcite is suggested, with gypsum as intermediate of the reaction. The Raman bands of the main compound in each spectrum are indicated [Colour figure can be viewed at wileyonlinelibrary.com]

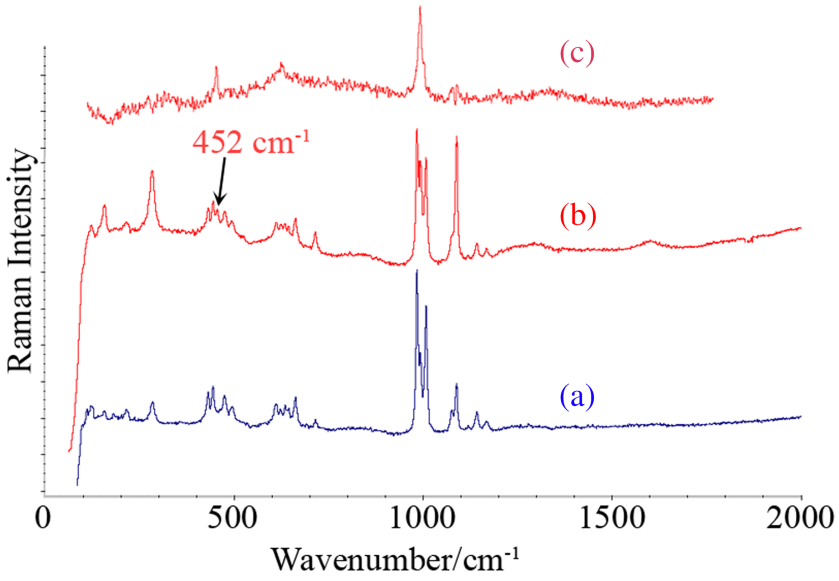

FIGURE 4 (a) Raman spectrum of a mixture of syngenite, thaumasite, and calcite; (b) Raman spectrum with a new band at 452 cm^{-1}; and (c) aphthitalite spectrum obtained after spectral treatment [Colour figure can be viewed at wileyonlinelibrary.com]

The formation of syngenite is clearly related to the gypsum presence as it has been demonstrated and to the reactivity of the materials. Thus, although syngenite is not related to a specific damage in the materials, as opposed to what happens with other compounds such as thaumasite or thenardite, whose identification remarks an important sulfating of the materials, and therefore, it could be act as pointer of the pollution of the building.

Regarding to thaumasite formation, this salt is commonly found in mortar and concrete because of an excessive sulfation. In the setting time, the sulfates react with concrete compounds as C_3A (tricalcium aluminate) to form ettringite ($Ca_6Al_2(OH)_{12}(SO_4)_3$—$26H_2O$) and monosulfoaluminate ($Ca_4Al_2(OH)_{12}SO_4$—$6H_2O$). Nevertheless, ettringite could keep reacting with the carbonated concrete and sulfates to form thaumasite ($Ca_6Si_2(OH)_{12}(CO_3)_2(SO_4)_2$—$24H_2O$) which is the most dangerous deterioration for the concrete. On the one hand, this salt is formed by a denominated expansive reaction due to the change of volume associated to it, promoting material cracks as in the case of thenardite and steel oxidation. On the other hand, thaumasite could continue reacting with the calcium hydrated silicate (CaO—SiO_2—H_2O, C-S-H) of the concrete until its complete disintegration.[53–55] That reactions could occur in the first hours of the cement application, but if thaumasite is formed later, it involves the presence of sulfates in the environment, but also of carbonates and water. So its identification is very relevant, since it indicates the simultaneous presence of sulfates and carbonates in the medium. Taking into account the mentioned facts, the identification of this salt is crucial for the risk assessment of the building because the most probable origin is the action of atmospheric pollution. The differentiation of thaumasite from ettringite or monosulfoaluminate is quite complex when their secondary bands are not present. However, in this case study, the characteristic bands of thaumasite at 1,074 and 659 cm^{-1} were clearly observed.[56] Overall, the presence of these kinds of compounds formed by the previous concrete carbonation and a subsequent atmospheric SO_2 attack are the most important affection suffered by the studied building, which is fixing the atmospheric pollutants in its materials.

According to the thenardite formation in efflorescences, it could be related to marine aerosol, rich in sodium, reacting with the atmospheric SO_2.[57,58] Generally, the reaction between this gas and marine aerosol forms thenardite, and it is deposited as this compound, or the marine aerosol can be deposited first and then the reaction takes place. The second way is more damaging because it could generate acid media which could affect the near materials. Nonetheless, thenardite could also be formed by a first carbonation and the subsequent sulfation of Na_2O, present in the original composition of the materials.[59] Anyway, in all the cases, atmospheric SO_2 attack is necessary.

Finally, the results of brick samples analysis revealed different original compounds as a potassium feldspar ($KAlSi_3O_8$, identified Raman bands at 513, 473, 282, and 155 cm^{-1}), quartz (SiO_2, main Raman band at 463 cm^{-1}), or anatase (TiO_2 orthorhombic, detected Raman bands at 636, 512, 395, 198, and 146 cm^{-1}) (Figure 5). This last compound is sometimes added to bricks as colorant, and it could be present in other two polymorphic forms: brookite (orthorhombic) and rutile (tetragonal). The anatase form is the most stable phase even when acids are

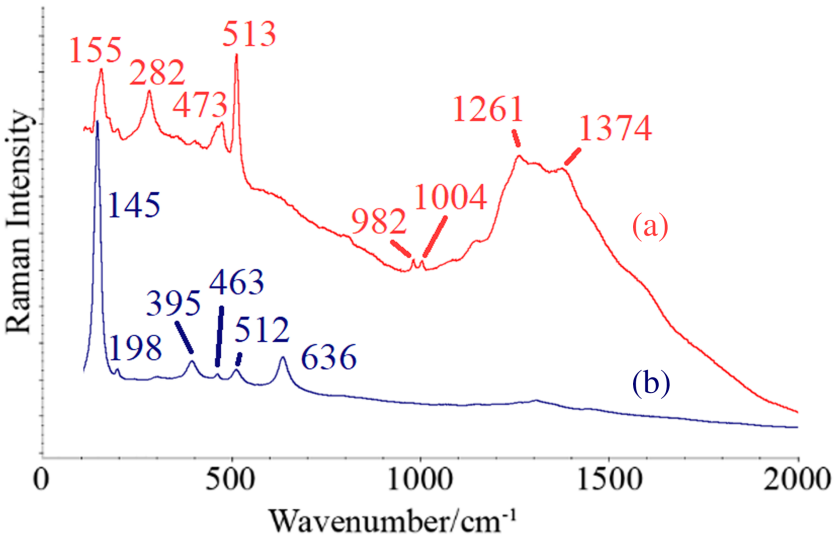

FIGURE 5 (a) Raman spectrum of potassium feldspar with syngenite; (b) Raman spectrum of anatase and quartz [Colour figure can be viewed at wileyonlinelibrary.com]

present. However, at higher temperatures than 400°C, it is transformed into rutile. This temperature could be increased up to 1,000°C depending on different variables as impurities.[60–63] Considering that the correct baking of bricks requires temperatures between 900°C and 1,150°C,[64–66] the detection of one of other polymorph would be an indicator of the temperature reached during the bricks manufacture. This is an important point, because the correct baking process guarantees an adequate vitrification of the components, improving the resistance of the bricks to environmental stressors by decreasing the capillary net.[64,66] Therefore, the identification of anatase instead of rutile indicated that the heating temperature of the brick had not been adequate. Probably, this was the reason of the bad conservation state of the bricks, mainly affected by salts. In this way, the Raman spectroscopy analysis pointed to syngenite as the principal decaying salt. This compound is formed through the carbonation and sulfation of the original calcium oxide, CaO, present in bricks by the action of atmospheric acid gases and promoted by the bad heating process.[67]

4 | CONCLUSIONS

The proposed methodology allowed identifying the affections suffered by the building in a rapid and reliable way, providing information during the in situ analysis, which improves the anticipation and responsiveness in the restoration process. The sampling in layers assisted by the in situ analysis permitted to collect representative samples and, at the same time, decreasing the amount of the samples collected, which is a very important factor in Built Heritage, but also in the forthcoming restoration works of modern buildings affected by environmental stressors. Moreover, thanks to this kind of sampling, the laboratory analysis was more effective, as well as faster. On the other hand, the guidelines offered are useful to solve problems in the spectra identification without the use of complementary techniques.

Regarding to the building affections, the Raman spectroscopy results pointed to the atmospheric acid gases (CO_2, SO_2, and NO_x) as principal stressors, being the SO_2 gas especially pronounced and accumulated in the building materials which could be a problem in the manipulation and recycling of the materials. In addition, gypsum seems to have an important role as intermediate in degradation processes, which pointed to this compound to be specially controlled. Besides, this methodology allowed not only external agents to be identified as deterioration sources, but also problems related to the materials quality, such as the low resistance of bricks because of low heating temperatures.

Overall, the present work demonstrates the viability of a new protocol based on a previous screening by in situ Raman spectroscopy analysis, a posterior layer sampling based on these results, and a final exhaustive Raman spectroscopy laboratory analysis. This methodology obtains the maximum information without the use of any complementary techniques which could be applied in common restoration works of urban buildings. Thus, this work points out how Raman spectroscopy is a very useful technique for the evaluation of the cement-based materials not only in the research field but also in restoration works which very satisfactory results.

ACKNOWLEDGMENTS

This work has been supported by the DEMORA (Grant No. PID2020-113391GB-I00) projects funded by the Spanish Agency for Research AEI (MICINN/FEDER-UE). O. Gómez-Laserna is grateful to the University of the

Basque Country (UPV/EHU) for her post-doctoral contract. The author wishes to acknowledge professional support of the Interdisciplinary Thematic Platform from CSIC Open Heritage: Research and Society (PTI-PAIS).

ORCID

Nagore Prieto-Taboada https://orcid.org/0000-0003-4649-2381
Olivia Gómez-Laserna https://orcid.org/0000-0002-2723-3168
Juan Manuel Madariaga https://orcid.org/0000-0002-1685-6335

REFERENCES

[1] O. Gómez-Laserna, M. A. Olazabal, H. Morillas, N. Prieto-Taboada, I. Martínez-Arkarazo, G. Arana, J. M. Madariaga, *J. Raman. Spectrosc.* **2013**, *44*, 1277.
[2] N. Prieto-Taboada, O. Gómez-Laserna, I. Ibarrondo, I. Martinez-Arkarazo, M. A. Olazabal, J. M. Madariaga, In Conference on Micro-Raman and Luminiscence Studies in the earth and planetary sciences (CORALS II), (Ed: Lunar and Planetary Institute), Lunar and Planetary Institute (LPI) y Consejo Superior de Investigaciones Científicas (CSIC), Houston, **2011**, 66.
[3] C. Riontino, C. Sabbioni, N. Ghedini, G. Zappia, G. Gobbi, O. Favoni, *Thermochim. Acta* **1998**, *321*, 215.
[4] P. Brimblecombe, *The Effects of Air Pollution on the Built Environment*, Imperial College Press, London **2003**.
[5] F. Gázquez, F. Rull, J. Medina, A. Sanz-Arranz, C. Sanz, *Environ. Sci. Pollut. Res.* **2015**, *22*, 15677.
[6] N. Prieto-Taboada, I. Ibarrondo, O. Gómez-Laserna, I. Martinez-Arkarazo, M. A. Olazabal, J. M. Madariaga, *J. Hazard. Mater.* **2013**, *248-249*, 451.
[7] N. Prieto-Taboada, C. Isca, I. Martínez-Arkarazo, A. Casoli, M. A. Olazabal, G. Arana, J. M. Madariaga, *Environ. Sci. Pollut. Res.* **2014**, *21*, 12518.
[8] E. Smith, G. Dent, *Modern Raman Spectroscopy—A Practical Approach*, John Wiley & Sons, Chichester (UK) **2005**.
[9] D. S. Moore, R. J. Scharff, *Anal. Bioanal. Chem.* **2008**, *393*, 1571.
[10] D. S. Moore, S. D. McGrane, *J. Mol. Struct.* **2003**, *661-662*, 561.
[11] J. M. Madariaga, *J. Raman, Spectrosc.* **2010**, *41*, 1389.
[12] A. Deneckere, B. Vekemans, L. Voorde, P. Paepe, L. Vincze, L. Moens, P. Vandenabeele, *Appl. Phys. A-Mater.* **2012**, *106*, 363.
[13] R. P. S. de Campos, I. V. P. Yoshida, M. C. Breitkreitz, R. J. Poppi, J. A. Fracassi da Silva, *Spectrochim. Acta a* **2013**, *100*, 67.
[14] R. Salzer, H. W. Siesler, *Infrared and Raman Spectroscopic Imaging*, Wiley, Mörlenbach (Germany) **2009**.
[15] N. Prieto-Taboada, O. Gómez-Laserna, I. Martinez-Arkarazo, M. Á. Olazabal, J. M. Madariaga, *Anal. Chem.* **2013**, *85*, 9501.
[16] P. Vandenabeele, *Practical Raman Spectroscopy: An Introduction*, Wiley, Chichester (UK) **2013**.
[17] C. M. Belfiore, D. Barca, A. Bonazza, V. Comite, M. F. Russa, A. Pezzino, S. A. Ruffolo, C. Sabbioni, *Environ. Sci. Pollut. Res.* **2013**, *20*, 8848.
[18] C. Tang, T. Ling, K. H. Mo, *Constr. Build. Mater.* **2021**, *268*, 121079.
[19] Y. Yue, J. J. Wang, P. A. M. Basheer, J. J. Boland, Y. Bai, *Constr. Build. Mater.* **2017**, *135*, 369.
[20] M. Vetter, J. Gonzalez-Rodriguez, E. Nauha, T. Kerr, *Constr. Build. Mater.* **2019**, *204*, 450.
[21] S. S. Potgieter-Vermaak, R. H. M. Godoi, R. V. Grieken, J. H. Potgieter, M. Oujja, M. Castillejo, *Spectrochim. Acta a* **2005**, *61*, 2460.
[22] N. Prieto-Taboada, M. Maguregui, I. Martinez-Arkarazo, M. Olazabal, G. Arana, J. M. Madariaga, *Anal. Bioanal. Chem.* **2011**, *399*, 2949.
[23] L. Bertrand, L. Robinet, M. Thoury, K. Janssens, S. Cohen, S. Schöder, *Appl. Phys. A-Mater.* **2012**, *106*, 377.
[24] O. Gómez-Laserna, N. Prieto-Taboada, I. Ibarrondo, I. Martinez-Arkarazo, M. A. Olazabal, J. M. Madariaga, in *Brick and Mortar Research*, (Eds: S. M. Rivera, A. L. Pena Diaz), Nova Science Publishers, New York, United States **2012** 195.
[25] A. Tournié, L. C. Prinsloo, C. Paris, P. Colomban, B. Smith, *J. Raman, Spectrosc.* **2011**, *42*, 399.
[26] P. Colomban, *J. Raman, Spectrosc.* **2012**, *43*, 1529.
[27] A. Sarmiento, M. Maguregui, I. Martínez-Arkarazo, M. Angulo, K. Castro, M. A. Olazábal, L. Á. Fernández, M. D. Rodríguez-Laso, A. M. Mujika, J. Gómez, J. M. Madariaga, *J. Raman, Spectrosc.* **2008**, *39*, 1042.
[28] R. Alberti, V. Crupi, R. Frontoni, G. Galli, M. F. La Russa, M. Licchelli, D. Majolino, M. Malagodi, B. Rossi, S. A. Ruffolo, V. Venuti, *J. Anal. At. Spectrom.* **2017**, *32*, 117.
[29] V. Crupi, G. Galli, M. F. La Russa, F. Longo, G. Maisano, D. Majolino, M. Malagodi, A. Pezzino, M. Ricca, B. Rossi, S. A. Ruffolo, V. Venuti, *Appl. Surf. Sci.* **2015**, *349*, 924.
[30] R. Masmoudi, K. Kupwade-Patil, A. Bumajdad, O. Büyüköztürk, *Constr. Build. Mater.* **2017**, *148*, 444.
[31] N. Prieto-Taboada, S. Fdez-Ortiz de Vallejuelo, M. Veneranda, I. Marcaida, H. Morillas, M. Maguregui, K. Castro, E. De Carolis, M. Osanna, J. M. Madariaga, *Sci. Rep.* **2017**, *8*, 1.
[32] A. Iturregui, N. Arrieta, J. Aramendia, I. Arrizabalaga, X. Murelaga, J. I. Baceta, M. Á. Olazabal, I. Martínez-Arkarazo, J. M. Madariaga, *J. Raman, Spectrosc.* **2016**, *47*, 329.
[33] I. Ibarrondo, U. Balziskueta, I. Martínez-Arkarazo, C. García-Florentino, G. Arana, A. Azkarate, J. M. Madariaga, *J. Raman, Spectrosc.* **2021**, *52*, 109.
[34] C. García-Florentino, M. Maguregui, H. Morillas, U. Balziskueta, A. Azcarate, G. Arana, J. M. Madariaga, *J. Raman, Spectrosc.* **2016**, *47*, 1458.
[35] M. Sawczak, A. Kamińska, G. Rabczuk, M. Ferretti, R. Jendrzejewski, G. Śliwiński, *Appl. Surf. Sci.* **2009**, *255*, 5542.
[36] T. D. Chaplin, R. J. H. Clark, M. Martinón-Torres, *J. Mol. Struct.* **2010**, *976*, 350.
[37] K. Castro, A. Sarmiento, M. Maguregui, I. Martínez-Arkarazo, N. Etxebarria, M. Angulo, M. Barrutia, J. González-Cembellín, J. Madariaga, *Anal. Bioanal. Chem.* **2008**, *392*, 755.
[38] M. L. Franquelo, A. Duran, L. K. Herrera, M. C. Jimenez de Haro, J. L. Perez-Rodriguez, *J. Mol. Struct.* **2009**, *924–926*, 404.
[39] S. Valadas, A. Candeias, J. Mirão, D. Tavares, J. Coroado, R. Simon, A. S. Silva, M. Gil, A. Guilherme, M. L. Carvalho, *Microsc. Microanal.* **2011**, *17*, 702.
[40] K. Castro, M. Pérez-Alonso, M. D. Rodríguez-Laso, L. Á. Fernández, J. M. Madariaga, *Anal. Bioanal. Chem.* **2005**, *382*, 248.

[41] M. Pérez-Alonso, K. Castro, J. M. Madariaga, *Curr. Anal. Chem.* **2006**, *2*, 89.
[42] P. Hewlett, *Lea's Chemistry of Cement and Concrete*, Elsevier Butterworth-Heinemann, New York (USA) **2003**.
[43] N. Prieto-Taboada, F.-O. de Vallejuelo, M. Veneranda, E. Lama, K. Castro, G. Arana, A. Larrañaga, J. M. Madariaga, *J. Raman Spectrosc.* **2019**, *50*, 175.
[44] N. Yoshida, Y. Matsunami, M. Nagayama, E. Sakai, *J. Adv. Concr. Tecnol.* **2010**, *8*, 121.
[45] M. Maguregui, A. Sarmiento, I. Martínez-Arkarazo, M. Angulo, K. Castro, G. Arana, N. Etxebarria, J. M. Madariaga, *Anal. Bioanal. Chem.* **2008**, *391*, 1361.
[46] M. Maguregui, K. Castro, H. Morillas, J. Trebolazabala, U. Knuutinen, R. Wiesinger, M. Schreiner, J. M. Madariaga, *Anal. Methods* **2014**, *6*, 372.
[47] J. Aramendia, L. Gomez-Nubla, K. Castro, I. Martinez-Arkarazo, D. Vega, A. de Sanz, A. de Garcia Ibáñez, J. M. Madariaga, *J. Raman Spectrosc* **2012**, *43*, 1111.
[48] N. Prieto-Taboada, O. Gómez-Laserna, I. Martinez-Arkarazo, M. A. Olazabal, J. M. Madariaga, *Anal. Chem.* **2014**, *86*, 10131.
[49] N. Prieto-Taboada, A. Larrañaga, O. Gómez-Laserna, I. Martínez-Arkarazo, M. A. Olazabal, J. M. Madariaga, *Microchem. J.* **2015**, *122*, 102.
[50] J. Stark, K. Bollmann, *Nordic Concrete Research* **2000**, *23*, 4.
[51] P. D. Tennis, S. Bhattacharja, W. A. Klemm, F. M. Miller, *Cem. Concr. Aggr.* **1999**, *21*, 212.
[52] S. Smillie, E. Moulin, F. P. Glasser, *Adv. Cem. Res.* **1993**, *5*, 93.
[53] S. Sahu, D. L. Exline, M. P. Nelson, *Cement. Concrete. Compos.* **2002**, *24*, 347.
[54] K. N. Jallad, M. Santhanam, M. D. Cohen, D. Ben-Amotz, *Cement. Concrete. Res.* **2001**, *31*, 953.
[55] H. Brocken, T. G. Nijland, *Constr. Build. Mater.* **2004**, *18*, 315.
[56] G. Renaudin, R. Segni, D. Mentel, J. Nedelec, F. Leroux, C. Taviot-Gueho, *J. Adv. Concr. Tecnol.* **2007**, *5*, 299.
[57] A. Chabas, R. A. Lefèvre, *Atmos. Environ.* **2000**, *34*, 225.
[58] N. Stefanis, P. Theoulakis, C. Pilinis, *Build. Environ.* **2009**, *44*, 260.
[59] P. W. Brown, A. Doerr, *Cem. Concr. Res.* **2000**, *30*, 411.
[60] K. P. Kumar, K. Keizer, A. J. Burggraaf, T. Okubo, H. Nagamoto, *J. Mater. Chem.* **1993**, *3*, 1151.
[61] Q. Gao, X. Wu, Y. Fan, *Dyes Pigm.* **2012**, *95*, 96.
[62] K. Yanagisawa, J. Ovenstone, *J. Phys. Chem. B* **1999**, *103*, 7781.
[63] S. R. Yoganarasimhan, C. N. R. Rao, *Trans. Faraday Soc.* **1962**, *58*, 1579.
[64] G. Cultrone, M. J. de la Torre, E. M. Sebastian, O. Cazalla, C. Rodriguez-Navarro, *Water, Air, Soil Pollut.* **2000**, *119*, 191.
[65] M. M. Jordán, A. Boix, T. Sanfeliu, C. de la Fuente, *Appl. Clay Sci.* **1999**, *14*, 225.
[66] I. González, E. Galán, A. Miras, *Appl. Clay Sci.* **2006**, *32*, 153.
[67] M. Maguregui, A. Sarmiento, R. Escribano, I. Martinez-Arkarazo, K. Castro, J. M. Madariaga, *Anal. Bioanal. Chem.* **2009**, *395*, 2119.

SUPPORTING INFORMATION

Additional supporting information may be found online in the Supporting Information section at the end of this article.

How to cite this article: N. Prieto-Taboada, O. Gómez-Laserna, I. Ibarrondo, I. Martinez-Arkarazo, K. Castro, G. Arana, María Ángeles Olazabal, I. Arrieta, J. M. Madariaga, *J Raman Spectrosc* **2021**, *52*(11), 1868. https://doi.org/10.1002/jrs.6217